applied sciences

MDPI

Article

Experimental Assessment of the Acoustic Performance of Nozzles Designed for Clean Agent Fire Suppression

Marco Strianese [1], Nicolò Torricelli [1,2], Luca Tarozzi [2] and Paolo E. Santangelo [1,3,*]

[1] Dipartimento di Scienze e Metodi dell'Ingegneria, Università degli Studi di Modena e Reggio Emilia, 42122 Reggio Emilia, Italy
[2] Bettati Antincendio S.r.l., 42124 Reggio Emilia, Italy
[3] Centro Interdipartimentale per la Ricerca InterMech—MO.RE., 41125 Modena, Italy
* Correspondence: paoloemilio.santangelo@unimore.it; Tel.: +39-0522-52-2223

Abstract: Discharge through nozzles used in gas-based fire protection of data centers may generate noise that causes the performance of hard drives to decay considerably; silent nozzles are employed to limit this harmful effect. This work focuses on proposing an experimental methodology to assess the impact of sound emitted by gaseous jets by comparing various nozzles under several operating conditions, together with relating that impact to design parameters. A setup was developed and repeatability of the experiments was evaluated; standard and silent nozzles were tested regarding the discharge of inert gases and halocarbon compounds. The ability of silent nozzles to contain the emitted noise—generally below the 110 dB reference threshold—was proven effective; a relationship between Reynolds number and peak noise level is suggested to support the reported increase in noise maxima as released flow rate increases. Hard drives with lower speed were the most affected. Spectral analysis was conducted, with sound at the higher frequency range causing performance decay even if lower than the acknowledged threshold. Independence of emitted noise from the selected clean agent was also observed in terms of released volumetric flow rate, yet the denser the fluid, the lower the generated noise under the same released mass flow rate.

Keywords: fire protection equipment; acoustic nozzle; inert gas; halocarbon compound; sound pressure level

Citation: Strianese, M.; Torricelli, N.; Tarozzi, L.; Santangelo, P.E. Experimental Assessment of the Acoustic Performance of Nozzles Designed for Clean Agent Fire Suppression. *Appl. Sci.* **2023**, *13*, 186. https://doi.org/10.3390/app13010186

Academic Editors: Giovanni Costantini and Daniele Casali

Received: 29 November 2022
Revised: 18 December 2022
Accepted: 20 December 2022
Published: 23 December 2022

1. Introduction

Several applications require gas-based fire protection systems, as the systems involving the discharge of liquid water—mainly those consisting of sprinklers—may cause damage to items that could even exceed the loss induced by the fire itself. One of the main examples, and also the reference case for the present work, is embodied by the protection of electrical and electronic equipment: any scenarios where an electrical voltage is applied (e.g., data centers) discourages the use of liquid water to perform fire suppression and extinction, since water exhibits high electrical conductivity [1,2]. Other typical scenarios consist of archives, libraries and generally all locations where the mentioned materials (e.g., paper) may be damaged by liquid water or where rapid cleanup after operating the system is recommended [1]. Prior to their 1994 ban as a result of the Montreal Protocol to protect the ozone layer [1], followed by a phase-out stage, halocarbon compounds, typically known as halons, were employed as gaseous agents, with Halon 1301 arguably being the most common. Their extinguishing action is primarily based on inhibiting the combustion reaction: the halogen atoms (i.e., bromine, chlorine or fluorine that substitute hydrogen within a compound derived from a hydrocarbon) react with chemicals involved in the combustion process, thus breaking its chain reaction [1]. Several substances are currently being used as halon replacements and are overall defined as clean agents [2]; they consist of either halocarbon compounds (e.g., the fluorinated ketone FK-5-1-12, also known as Novec, and employed in the present work) or inert gases (e.g., argon and nitrogen, also tested in the present research). The involved systems are total flooding: the whole compartment that is on fire is filled with the released gaseous agents. So, both categories mainly rely on oxygen depletion as their main extinguishing mechanism [2]; however, the former also tends to combine chemical action (i.e., inhibition of combustion) with heat extraction and, consequently, flame cooling towards extinction.

In spite of the numerous advantages exhibited by clean agents, the main form of which is characterized as being electrically non-conductive, leaving no residue after discharge and having virtually null Ozone Depletion Potential (ODP), the whole related system may be somewhat complex, since they require a storage capacity larger than that of halon-based systems as a result of poorer extinction effectiveness [2]. Most clean agent fire suppression systems include a storage tank, where the agent is superpressurized—usually by nitrogen—if in the form of a liquified gas, as is the case for most halocarbon compounds, or is simply contained at high pressure (usually in the range of 150–300 bar) in the case of an inert gas system [2,3]; valves, piping, nozzles and controllers (e.g., flow rate and pressure) are also part of the design. While the mechanical strength of pipes and nozzles to withstand the gas pressure does not currently appear a major concern for designers, the noise generated by the agent, mostly at the nozzle exit and, to a lesser extent, through valves and channels, represents a potentially relevant cause of damage to the equipment in the compartment, as well as first responders (e.g., firefighters) if present within the compartment as the discharge occurs [4]. A well-known problem and subject of extensive research efforts in aeronautics [5], the high-speed jet noise yielded by turbulence intensity at the nozzle outlet, and often emphasized by transitioning from subsonic to supersonic flow [6,7], has been studied for decades, mainly with the aim of reducing its intensity. In the case of clean agent gaseous jets released in a generic compartment undergoing a fire event, the sensitivity of Hard Disk Drives (HDDs) to noise can result in a remarkable performance loss [4,8]. As a quantitative experimental result, Sound Pressure Level (SPL) in the range of 110–130 dB is commonly accepted as the threshold beyond which HDD read/write performance becomes dramatically penalized [4,9,10]. Interestingly, HDD performance loss due to the overpressure and the steep pressure gradient caused by rapid discharge within the compartment appears somewhat irrelevant [4]. In spite of the increasing popularity of new technologies (e.g., Solid-State Disks—SDDs), which are not noise-sensitive, this problem may have a significant extent: in 2021, there were about 8000 data centers in the 110 countries providing information, with a predicted 150-fold increase in the generation of new data over the 2010–2025 timespan [11]. Moreover, a similar detrimental effect of noise yielded by the same gaseous jets can likely occur in some medical devices featuring an architecture similar to that of HDDs, an issue worth considering in fire protection systems designed for the healthcare industry.

As a technical solution to reduce the noise generated by clean agent discharge, silent nozzles—often also referred to as acoustic nozzles—have been developed. Since modifying the nozzle outlet does not appear to fully address the challenge, given that SPL was proven to be largely independent of nozzle shape [7], adding sound absorptive layers to the nozzle outer surface has become the most employed approach [3,12,13], with the insertion of horizontal plates also being recommended to make the released flow rate and pressure as balanced as possible in multiorifice nozzles [12,14]. Currently, the open literature presents relatively few studies that focus on the design of such nozzles and on assessing their acoustic performance, especially when compared with that exhibited by standard nozzles under the same discharge conditions. In that regard, it is worth mentioning that Koushik et al. [15] proposed an experimental approach to evaluate noise emitted by standard fire suppression nozzles releasing inert gases: an array of microphones were employed to measure SPL at various azimuthal locations with a constant distance (1 m) from the nozzle. Some degree of directionality (i.e., dependence on the angular coordinate) was found, together with potential impact of walls on the acoustic path (i.e., reflection and direct path). The extensive use of numerical modeling generally permeates the works on silent nozzles, most of which [12,14] are focused on determining the most effective nozzle selection and configuration within an enclosure towards making SPL at the HDD locations lower than the previously mentioned threshold (110–120 dB, in those studies). On the other hand, the more recent contributions by Kim et al. [3,13] present a computational approach—remarkably validated through dedicated experiments—to optimize some design parameters of silent nozzles. Guided by DOE (Design of Experiments), their research effort led to them identifying the diameter of the external sound-absorbing shell as the most impactful variable. It is worth noting that some of the reviewed works suggest a certain dependence of the emitted noise on the orientation of the nozzle and the location at which SPL is evaluated [14,15], whether the nozzle is a standard or a silent one; on the other hand, other studies appear to practically consider the nozzle as a point source [3,12]. This aspect may be mostly related to the nozzle geometry.

Even though some comparison between standard and silent nozzles is presented in the work by Loureiro et al. [12], it appears that a quantitative and comprehensive approach to the purpose represents a challenge still to be addressed, at least in the open literature. More specifically, an experimental methodology allowing investigators to carry out such a comparison in terms of variables of interest for fire protection system designers (e.g., type of clean agent, released flow rate, orifice diameter) is still in demand. The present research is aimed at embarking on this quest, with the experimental datasets and facilities provided and described in the studies by Kim et al. [3] and Loureiro et al. [12] serving as a foundation. Arguably an unprecedented effort, this work may set a standard methodology to quantitatively compare the acoustic performance of various standard and silent nozzles, also leading to discussion in reference to the relevant physical quantities. Both the proposed approach and the obtained results could be appealing to designers and researchers focusing on clean agent fire suppression.

2. Materials and Methods

As remarked in the introduction (Section 1), no standard procedure is currently available for testing the acoustic performance of nozzles used in gas-based fire suppression. However, some previous works [3,12] present the description of experimental rigs; moreover, some technical standards are also available on fire protection of data centers and electrical devices [16], together with technical reports about tests to evaluate the harmful effect of noise—notably that emitted by gaseous jets released through a nozzle—on HDDs [17–20]. Thus, both the setup and procedure developed and proposed here were inspired by these sources of information.

2.1. Experimental Setup and Procedure

The experimental setup was installed in a large enclosure (25 × 10 × 5 m, length × width × height); a sketch of the whole assembly is presented in Figure 1. Aiming at evaluating acoustic performance of the nozzles against both categories of clean agents, the rig was designed to accommodate the storage and the supply system of both nitrogen IG100, employed as representative of the inert gases, and FK-5-1-12, employed as representative of halocarbon compounds. In fact, this selection required us to assemble two facilities, due to the different nature and properties of the two involved substances: the first rig was used to discharge a plain inert gas (i.e., nitrogen IG100), as shown in Figure 1a; the second rig was devised to discharge a multiphase, bicomponent mixture (i.e., FK-5-1-12 and nitrogen), as shown in Figure 1b. Since FK-5-1-12 is stored as a liquified gas, nitrogen was required to pressurize it within its storage tank (Section 1).

As demonstrated in Figure 1, the difference between the two testing facilities lies in the supply system (i.e., storage and piping), which required setting different lengths of the pipes and selecting components made of different materials.

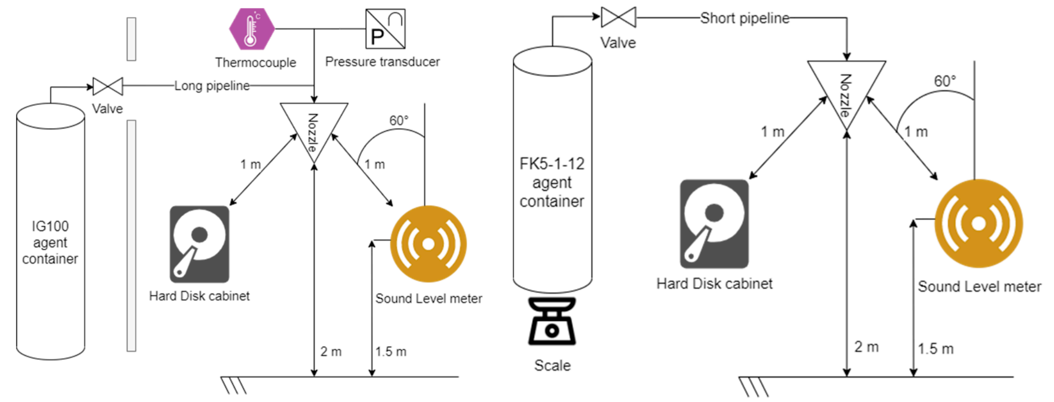

(a) (b)

Figure 1. Schematic of the realized setup to evaluate acoustic performance by supplying (**a**) nitrogen IG100 or (**b**) FK-5-1-12.

Notably, the first setup (Figure 1a, used for the plain inert gas) featured a longer pipeline (10 m) and a constant flow valve manufactured by Bettati Antincendio S.r.l. (Reggio Emilia, Italy) to allow the regulation of the supplied flow rate. The longer length of the pipes were designed to accommodate the storage container and the related valve in a separate room, hence the wall sketched in Figure 1a, since the employed valve represents an additional source of noise, which would have biased the comparison between the inert gas and the halocarbon compound configurations, if not conveniently offset. As also included in Figure 1a, the facility for inert gas discharge was provided with a thermocouple and a pressure transducer, inserted within the pipeline at 200 mm distance from the nozzle (i.e., about 5–10 times the maximum diameter of the orifices used throughout the experiments [21]). These instruments were required to measure temperature and pressure of the gas stream as an input to ultimately calculate the released mass flow rate through the relationships reported in Section 2.2. On the other hand, these probes were not included within the facility for FK-5-1-12 discharge (Figure 1b), since their multiphase nature does not allow an evaluation of the supplied flow rate by any suitable model. Therefore, mass was recorded using a scale directly placed under the storage cylinder, then reconstructing mass flow rate through a finite difference approximation, also described in Section 2.2. The facility for FK-5-1-12 discharge featured a shorter pipeline (1.5 m) connecting the container to the nozzle, as the valve employed in this case, also manufactured by Bettati Antincendio S.r.l., did not contribute significantly to noise generation.

It is worth clarifying that the temperature and pressure of the substances contained in the storage cylinders were monitored in both facilities, as well as directly downstream of the valve: in the former case, the tank included a pressure gauge and a thermocouple, whereas in the latter, another pressure transducer and thermocouple were inserted. The tank used for hosting nitrogen IG100 featured 80 L capacity, with gas being stored at 300 bar pressure; the valve allowed regulating outlet pressure to impose 70 bar maximum pressure in the manifold. FK-5-1-12 was stored in a 14 L tank instead, with a 1 kg/L filling ratio (i.e., 1 kg of clean agent per 1 L storage capacity). As typical in the storage of liquified gases, the agent was superpressurized at 70 bar by nitrogen; the employed valve was specifically developed to issue a flow at 42–70 bar. A full view of the setup is shown in the photo of Figure 2, which combines and includes all the items of both facilities.

The nozzle was placed at the center of the base of the chamber, as far away from the walls as possible. This configuration—applied within a large enclosure—was aimed at reducing the effect of reverberation by walls, which was assessed as potentially significant [15], since the tests were not conducted in an anechoic chamber.

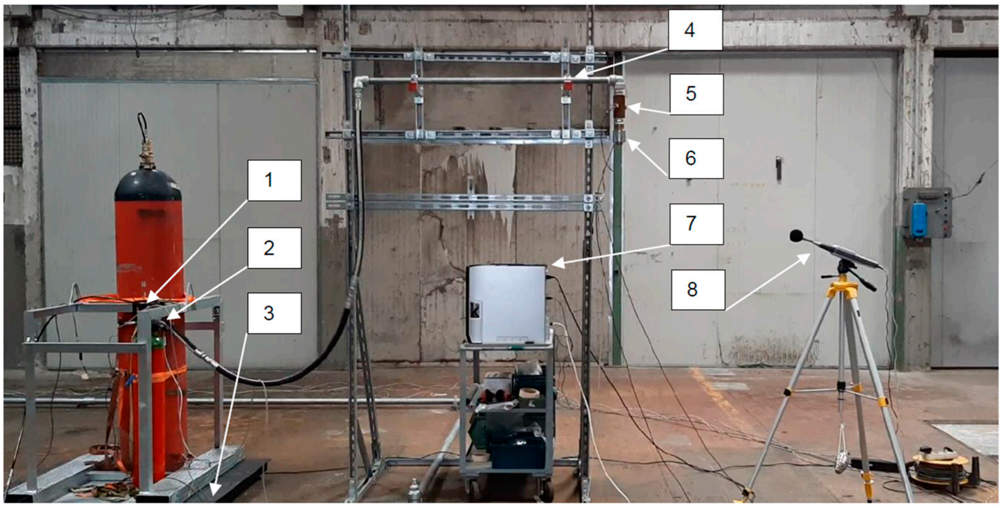

Figure 2. Photo of the experimental setup: (**1**) storage cylinder; (**2**) pressure transducer and thermocouple (downstream of the valve); (**3**) scale; (**4**) pipeline; (**5**) pressure transducer and thermocouple (upstream of the nozzle, only for inert gas discharge system); (**6**) nozzle; (**7**) servers, including one SSD and two HDD; (**8**) sound level meter.

The nozzle was also placed at 2 m height from the floor (Figure 1), a common value in installations within data centers [16] and suitable for accommodating all the components surrounding it. As for nozzle types, the tested ones are all manufactured by Bettati Antincendio S.r.l.: Figure 3 presents photos of both the employed standard nozzle (Figure 3a) and silent ones designed for each category of clean agents (Figure 3b,c).

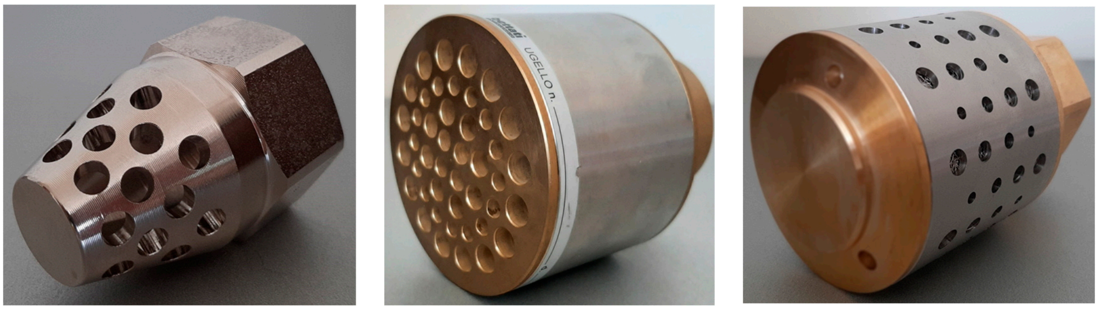

(**a**) (**b**) (**c**)

Figure 3. Photos of the nozzles employed in the experiments: (**a**) standard; (**b**) silent nozzle for the discharge of inert gases; (**c**) silent nozzle for the discharge of halocarbon compounds (low ceiling height).

Interestingly, some preliminary tests made select a silent nozzle for low ceiling installations (Figure 3b) when the discharge of halocarbon compounds (i.e., the FK-5-1-12) was involved, since it proved more effective, especially if combined with the chosen valve. On the other hand, silent nozzles were employed in the discharge of nitrogen IG100. It is worth clarifying that the tested silent nozzles present a sound-absorbent layer included within their frame, which makes them similar to those investigated in the works by Kim et al. [3,13]. Figure 4 presents simplified technical sketches of the employed nozzles, highlighting the orifice diameter.

As shown in Figure 4b,c, silent nozzles are endowed with the mentioned sound-absorbing shell. Orifice diameter varied over the following values in the whole series of tests and for both standard and silent nozzles: 5, 6, 10, 14, 17 and 23 mm. It is worth clarifying that the experimental setup proposed in the present work is aimed at comparing standard with silent nozzles in a single-nozzle configuration. Therefore, the combined action of the discharge by more nozzles at the same time, and its effect on noise, is not included; notably, superposition of waves and interference of sound may make the generated noise vary from that produced by a single nozzle throughout its discharge.

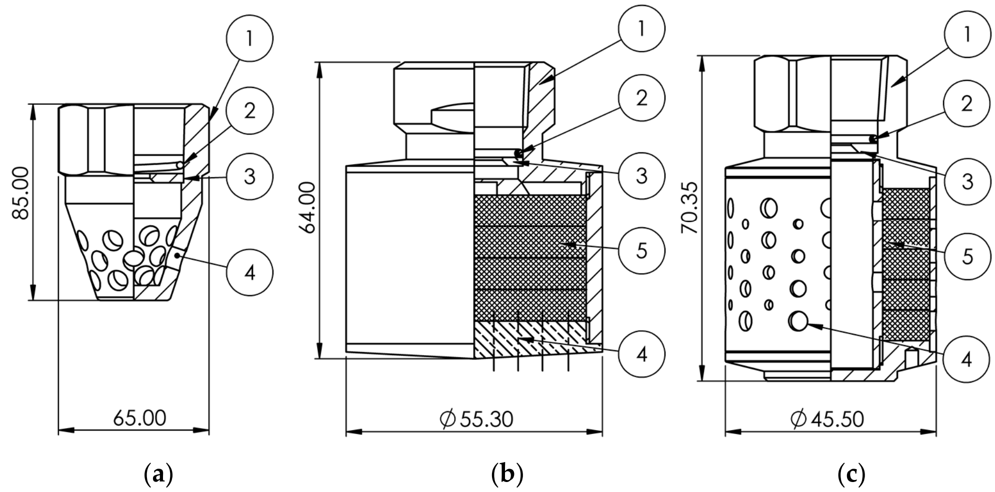

Figure 4. Technical sketch of the employed nozzles, with values provided referring to the orifice diameter: (**a**) standard; (**b**) silent; (**c**) silent for low ceiling applications; the marked components are (**1**) nozzle body; (**2**) spring; (**3**) orifice; (**4**) holes; (**5**) sound-absorbing layer.

A server rack containing an SSD and two HDDs with different characteristics was located at 1 m distance from the nozzle outlet (Figure 1) to assess the impact of the emitted noise on electronic equipment typical of data centers. The set distance is consistent with that applied in previous works [12,15] for evaluating SPL from nozzles used in gas-based fire suppression.

Both HDD and SSD performance was evaluated by recording their speed over time using a free software (*HD Speed* version 1.7, released by SteelBytes). The acoustic emissions from the tested nozzles were measured by a sound level meter, with its microphone positioned at 1 m distance from the nozzle exit and at 1.5 m from the floor (Figure 1); the instrument (specifically, its axis of symmetry) was inclined by about 60 °C with respect to the vertical axis, coincident with the axis of symmetry of the nozzle. The distance between the sound level meter and the nozzle is consistent with the value set for the server rack, and also supported by previous studies [12,15] and recommendations from test reports [17–20], since it is representative of the typical minimum distance at which obstructions (e.g., a cabinet containing electronic equipment) are located.

The measuring instruments employed in the experiments and their characteristics (e.g., acquisition frequency, accuracy) are summarized in Table 1; the characteristics of the used hard drives—both HDD and SDD—are reported in Table 2, with specific focus on rate of rotation (HDD only) and nominal speed.

Table 1. Employed measuring instruments and relevant characteristics.

Measured Parameter	Acquisition Frequency (Hz)	Instrument/ Sensor	Data Acquisition Board
Storage mass (cylinder + clean agent)	10	Scale *P1250S5* by LAUMAS Elettronica, 1500 kg F.S.	*NI 9208* board by National Instruments, 16 channels (current)
Pressure	10	Pressure transducer *21y* by Keller, 400 bar F.S. ± 0.1 bar accuracy	

Table 1. *Cont.*

Measured Parameter	Acquisition Frequency (Hz)	Instrument/ Sensor	Data Acquisition Board
Temperature	10	Thermocouple T type, 1.0 mm bead diameter, accuracy in accordance with standard IEC 60584	*NI 9212* board by National Instruments, 8 channels (thermocouple)
SPL	1	Sound level meter *HD2010UC/A* by Deltaohm, with spectral analysis by octave bands from 31.5 Hz to 8 kHz	Data stored on the instrument
Hard drive performance	2	–	Data recorded by *HD Speed* software, version 1.7

Table 2. Employed hard drives and relevant characteristics (*, assessed in a quiet room using *HDSpeed* software).

Reference Name	Manufacturer	Model	Type	Rate of Rotation (rpm)	Nominal Speed * (MB/s)
SSD	Toshiba	*OCZ-VERT EX3 MI SCSI*	SSD	–	229
HDD1	Hitachi	*DeskStar 7K160*	HDD	7200	77
HDD2	Western Digital	*WD36 ADFD*	HDD	10,000	89

The tested configurations are reported in Table 3. Notably, the performed experiments can be subdivided into three types, all of which were conducted on both standard and silent nozzles:

- The first set was aimed at assessing the reliability of the experimental setup and measurements—mostly through statistical analysis—together with evaluating the potential directionality of SPL; these tests were carried out employing an inert gas mixture (i.e., IG55, 50% argon and 50% nitrogen) with a fixed nozzle diameter (5 mm) and pressure at the nozzle outlet; measurements were taken at various values of the distance between the nozzle and the sound level meter, also varying the angle of inclination of the sound level meter with respect to the nozzle.
- The second set was aimed at investigating the discharge of inert gases (nitrogen IG100, in the present case); these tests were carried out at varied orifice diameters, between 5 and 23 mm, while keeping the distance between the nozzle and the sound level meter constant and equal to 1 m (Figure 1).
- The third set was aimed at investigating the discharge of halocarbon compounds (FK-5-1-12, in the present case); these tests were carried out only using nozzles with 6 mm orifice diameter, given the higher cost of the involved substance; the distance between the nozzle and the sound level meter was also kept constant and equal to 1 m (Figure 1).

At least three repeated tests were conducted for each configuration listed in Table 3 to acquire a statistically significant dataset.

Table 3. Detailed list of the investigated configurations (*, multiple data series recorded for each tested distance at various angular locations).

Set	Nozzle Type	Clean Agent	Nozzle-to-Sound Meter Level Distance (m)	Nozzle Diameter (mm)
I	Silent	IG55	2.5	5
	Silent	IG55	1.25	5
	Silent	IG55	5	5
	Silent	IG55	1–2–4–8 *	5
	Standard	IG55	1–2–4–8 *	5
II	Silent	IG100	1	5
	Standard	IG100	1	5
	Silent	IG100	1	10
	Standard	IG100	1	10
	Silent	IG100	1	14
	Standard	IG100	1	14
	Silent	IG100	1	17
	Standard	IG100	1	17
	Silent (low ceiling applications)	IG100	1	17
	Silent	IG100	1	23
	Standard	IG100	1	23
III	Standard	FK-5-1-12	1	6
	Silent (low ceiling applications)	FK-5-1-12	1	6

2.2. Data Processing and Analysis

The analysis of the acquired experimental dataset pursued two main purposes through dedicated approaches:

- Determining and comparing the acoustic performance of standard and silent nozzles; to this end, SPL is presented as a function of released flow rate and time for both tested clean agents and for the whole set of investigated orifice diameters; the results from spectral analysis by octave bands are also included.
- Evaluating the effect of SPL on the different tested hard drives and highlighting quantitatively the performance loss in the same configuration towards a comparison between standard and silent nozzles; to this end, an index of the disk behavior and performance through the discharge is proposed as inspired by a recent report [20], which produces measurements of read/write speed and includes that under the SPL due to white noise (i.e., baseline speed).

$$Disk\ performance\ index = \frac{Disk\ speed}{Disk\ baseline\ speed}. \quad (1)$$

Moreover, the reliability of the acquired dataset and the overall experimental approach was challenged by the following:

- Checking the applicability of the point source model [22], which supports the proposed design of the experimental setup, where SPL was measured at the location described in Section 2.1 and shown in Figure 1, without resorting to an array of microphones, as in [15]; this preliminary evaluation is included in Section 2.3.
- Evaluating standard deviation [23] of the acquired data—mainly the SPL dataset as a function of time or released flow rate over repeated tests under the same configuration—in order to assess repeatability.

As already mentioned in Section 2.1, the released flow rate was calculated for both the inert gas and the halocarbon compound discharge. Notably, a classic model was employed to calculate the former, with the flow rate of a jet (compressible flow, assuming an ideal gas) issued through an orifice [24] being expressed by Equation (2):

$$\dot{Q}_m = \gamma \cdot A_m \cdot \rho_{m,CR} \cdot w_{m,CR}, \text{ if } \beta_{noz} \le \beta_{CR}, \\ \dot{Q}_m = \gamma \cdot A_m \cdot \sqrt{\frac{2k}{k-1} \cdot p_0 \cdot \rho_0 \left({\beta_{noz}}^{\frac{2}{k}} - {\beta_{noz}}^{\frac{k+1}{k}} \right)}, \text{ if } \beta_{noz} > \beta_{CR}, \tag{2}$$

where $\dot{Q}_m$ is mass flow rate, γ is the discharge coefficient of the nozzle, A_m is the surface area of the outlet section, ρ is density, w is the average jet velocity, β is defined as the ratio between pressure downstream of the nozzle (i.e., atmospheric pressure) and upstream of the nozzle, $w_{m,CR}$ refers to the gas velocity at nozzle orifice, CR refers to critical value of air at 20 °C temperature and noz refers to nozzle. The following set of relationships allows the quantification of discharge coefficient, density and velocity, through the jet temperature:

$$\gamma = e^{k1} \cdot p_0^{k2} \cdot D_m^{k3}, \tag{3}$$

$$\rho_{m,CR} = \rho_0 \cdot \left(\frac{2}{k+1} \right)^{\frac{k}{k-1}}, \tag{4}$$

$$w_{m,CR} = \sqrt{k \cdot R_{gas} \cdot T_{m,CR}}, \tag{5}$$

$$T_{m,CR} = T_0 \frac{2}{k+1}, \tag{6}$$

where e is the Euler's number, p is gas pressure, D_m is the orifice outlet diameter, 0 refers to the conditions upstream of the nozzle, k is defined as the ratio between specific heat capacity at constant pressure and specific heat capacity at constant volume of the involved gas, R_{gas} is the specific gas constant, T_m is jet temperature, T is temperature and $k1$, $k2$ and $k3$ are coefficients specific to the nozzle. Density values were taken from the *CoolProp* free library [25] by selecting that of nitrogen corresponding to temperature and pressure measured upstream of the nozzle (Section 2.1, Figure 1a). The $k1$, $k2$ and $k3$ coefficients were experimentally quantified by VdS Schadenverhütung GmbH for the selected nozzles, in order to also evaluate their outflow area.

The evaluation of mass flow rate in the case of the FK-5-1-12 discharge was performed by processing the readings of the employed scale (Section 2.1, Figure 1b). As previously mentioned, the derivative of mass with respect to time was calculated by the approximation of the differential to finite difference:

$$\dot{Q}_m = \frac{dm}{dt} \approx \frac{\Delta m}{\Delta t} = \frac{m_i - m_{i+1}}{\frac{1}{f}}, \tag{7}$$

where m is mass, t is time, f is acquisition frequency and i is the index referring to the generic ith acquisition (i = 0, . . . n, where n is the last but one acquisition). This approach is relatively common to extrapolate mass flow rate from mass readings [26–28]; no moving average was applied in this calculation, since the acquired mass trend proved relatively bias-free in terms of statistical noise.

2.3. Applicability of Point Source Model and Statistical Analysis

The point source model consists of assuming that sound radiates equally and symmetrically in all directions from the emitting source; as the underlying hypothesis, the source is far smaller than the wavelength associated with the emitted sound [22]. This spherical symmetry implies that sound intensity $I = W/4\pi r^2$, where W is the power in the wave and r is the radius of the generic sphere, decreases according to the classic inverse square law (i.e., $\sim 1/r^2$) as distance from the source increases. Sound pressure follows an inversely proportional law (i.e., $\sim 1/r$) instead; SPL expresses sound pressure relative to a reference value through a logarithmic function (i.e., $SPL = 20 \log(p/p_0)$, where p is sound pressure, 0 refers to the reference value, and the unit for SPL is dB). Combining the previously reviewed relationships, a quantitative result from the point source model consists of SPL decreasing by about 6 dB each time the distance from the emitting source is doubled.

The applicability of the point source model to the present case was challenged by a preliminary set of tests (i.e., the first set described in Section 2.1 and reported in Table 3). The scope was to evaluate the agreement between theory and experimental results, mainly by assessing the distance from the nozzle to the sound level meter at which sound absorption and reflection from walls make the approximation inevitably fail, and the degree of directionality. This latter parameter was investigated by varying the angle of inclination of the sound level meter with respect to the nozzle (i.e., the source) over several values in the 0–90 °C range, thus following the approach by Koushik et al. [15]. As reported in Table 3, the distance between source and instrument was also varied at each testing location over the angular coordinate. Figure 5 shows the SPL dataset acquired at various angular locations at the selected values of the distance (1, 2, 4 and 8 m from the nozzle).

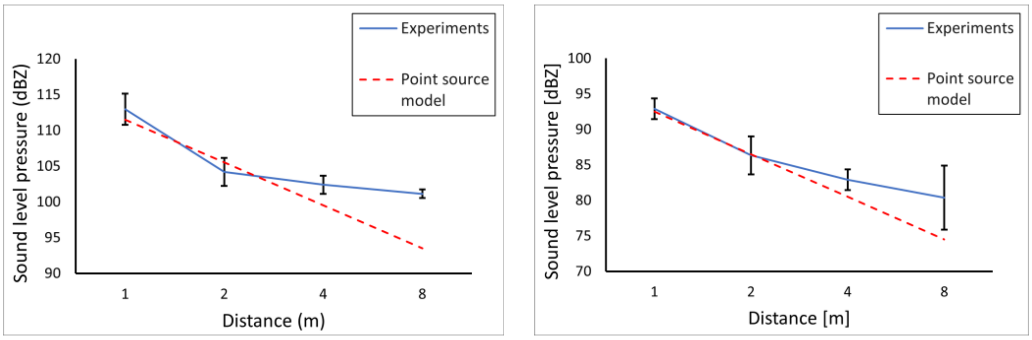

(**a**) (**b**)

Figure 5. Comparison experimental results and point source model at various values of nozzle-to-sound level meter distance for (**a**) standard and (**b**) silent nozzles; data points represent mean SPL value over the dataset acquired at the same distance and varying the angle of inclination; the error bars represent doubled standard deviation.

Notably, the data points represent the mean SPL value over the dataset collected at various angular locations at the same distance, while the error bar represents the doubled standard deviation calculated over the same population [23].

The SPL trend predicted by the point source model is also included. As demonstrated by the comparison between predicted and experimental profiles, the applicability of the model to the proposed experiment appears firmly supported within a 2 m diameter sphere centered at the nozzle as the source, for both standard (Figure 5a) and silent (Figure 5b) nozzles. On the other hand, as the distance is further increased, reverberation and absorption by walls appear to make the assumption of point source increasingly fail. As previously noted, point source theory relies on the complete absence of directionality, which is in fact somewhat present for both the standard (Figure 5a) and the silent nozzle (Figure 5b). However, the variability over the investigated angular locations at 1 and 2 m distance from the nozzle (i.e., those relatively free from the wall effect) is limited to ±2.5 dB: even though quantitatively not negligible, it was deemed small enough to allow the point source model to be reasonably applicable, even in light of a threshold distinguishing harmless from harmful noise to HDDs with a 20 dB span (110–130 dB, Section 1). Thus, the proposed experimental approach and setup (Section 2.1, Figure 1), where the sound pressure was evaluated at 1 m distance from the nozzle and hard drives were placed at the same distance to assess the impact of noise on their performance, appears overall supported for the nozzles tested in the present study.

As reported in Section 2.2, error analysis was also carried out to assess the repeatability of the experiments. This evaluation was also conducted through the first set of tests (Table 3); notably, specific experiments were performed at fixed pressure against both standard and silent nozzles, where 10 s sampling time was applied to SPL measurements, varying the distance from the nozzle. Figure 6 shows the dataset acquired at 1, 2 and 4 m distance from the nozzle over the 10 s acquisition (overall, five series of acquisitions); as a representative example, the tests conducted with the standard nozzle are considered in the graphic.

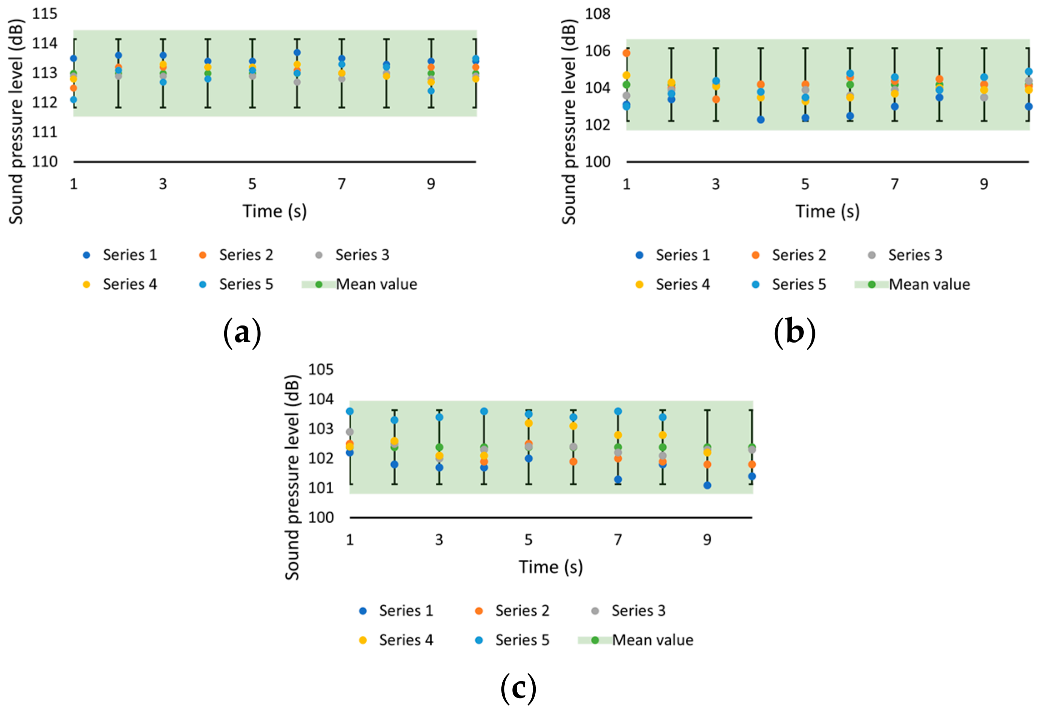

Figure 6. SPL dataset to assess the repeatability of the experiments for the standard nozzle, with data points collected at (**a**) 1, (**b**) 2 and (**c**) 4 m distance from the nozzle to the sound level meter.

The plot includes individual data points and mean values calculated at each acquisition, together with a band, the size of which is three times the maximum standard deviation calculated over the whole set of tests. All the data points lie within the highlighted band, which exhibits relatively high repeatability and low random error (i.e., high precision). From a quantitative standpoint, the standard deviation calculated for the dataset shown in Figure 6 is in the order of 0.5–1 dB, which amounts to less than 1% of the reading. As mentioned in Section 2.1, the first set of tests specifically served as a source of data for statistical analysis. However, the assessment of variance should be taken as representative of repeatability for the whole set of experiments, since no significant difference from the value previously reported arose when performing similar analysis against the dataset from the second and the third set of tests.

3. Results and Discussion

In this section, the outcomes from the experiments conducted through the second and the third set of tests (Table 3) are presented and discussed, mostly focusing on the comparison between standard and silent nozzle in terms of acoustic performance and detrimental effect on the read/write speed of the selected hard drives. An evaluation of the impact of design parameters such as orifice diameter, released clean agent and released mass flow rate also stemmed from this comparison.

3.1. Discharge of Inert Gases: Effect of Generated Noise

The diagrams included in Figure 7 show the effect of the noise generated by standard and silent nozzles with various orifice diameters on both HDDs and SDDs, throughout a full discharge of nitrogen IG100. Notably, selected experiments using nozzles of 5, 10, 14, 17 and 23 mm diameter are presented; the results from the tests with the silent nozzles for low ceiling applications are omitted, as an approximately similar behavior was found between them and the other silent nozzles with the same orifice diameter. Overall, the experimental results demonstrate the ability of silent nozzles to bring SPL down to relatively harmless values through the discharge: standard nozzles present SPLs greater than 110 dB—the lower limit of the damaging threshold (Section 1)—over most of the gas release, and in most cases (i.e., for orifice diameter greater than 5 mm), peaks exceeding 120 dB occur; on the other hand, the SPL of silent nozzles exceeds the threshold only for about 25 s even with the larger orifice diameter (larger than 10 mm), also never reaching 120 dB. As a finding of general validity for both types of nozzle, SPL exhibits a sudden increase up to a local maximum upon starting the discharge, which is consistent with the theory associated with noise emitted by gaseous jets [5–7], reviewed in Section 1: since noise is largely due to turbulence effects, it may be interpreted as function of Reynolds number ($Re = w_{m,CR} D_m / v$, where v is kinematic viscosity of the involved substance); as Re increases, turbulence develops until critical Re is reached (i.e., fully developed turbulence) [29], to which SPL local peaks arguably correspond.

Instances of additional maxima occurring after the first peak appear mostly for the discharge through the standard nozzle (Figure 7a,c,d,e), and hint at some slight pressure variability imposed by the constant flow valve: constant flow valves are developed and employed to keep pressure and, consequently, flow rate as constant as possible throughout the discharge, which would virtually result in constant Re and SPL until pressure decays in the storage tank towards the end of the process. This practically translates into a plateau-like behavior, as apparent in Figure 7f,g,h, with the potential singularities previously mentioned occurring in some cases. The proposed discussion also substantiates another observation holding for both standard and silent nozzles (Figure 7): the larger orifice diameter, the higher the SPL maxima and overall SPL values throughout its trend.

Assuming constant pressure (i.e., 70 bar, as mentioned in Section 2.1), at least throughout the controlled phase of the discharge, results in almost constant average velocity, even with a Bernoulli inviscid model [30]; as orifice diameter increases, both Re and released mass flow rate increase. Therefore, it can be inferred that the discharge time obviously decreases, while SPL increases, as higher flow rate is issued, providing that supply pressure is kept constant.

An insight into the effect of the sound frequency stems from maps presenting SPL as a function of time and frequency throughout the discharge; Figure 8 shows experiments conducted for both standard and silent nozzles with 10, 17 and 23 mm orifice diameter as the most representative. It is interesting to note that SPL reaches higher values (i.e., greater than 110 dB) within the 1–8 kHz range, which is somewhat lower than the findings from Koushik et al. [15] on standard nozzles (i.e., more in the 10–20 kHz range). This suggests that the employed nozzles emit noise at lower frequency, hence higher wavelength, which ultimately yields more reliable applicability of the point source model (Section 2.3) as a result of the less remarkable directionality found with respect to the noise emitted by the nozzle used in [15]. Moreover, SPL appears higher than 100 dB over periods of time when frequency is greater than 4 kHz. According to Dutta [31], noise can affect hard drive performance even beyond a 105 dB threshold at a frequency between 4 and 10 kHz.

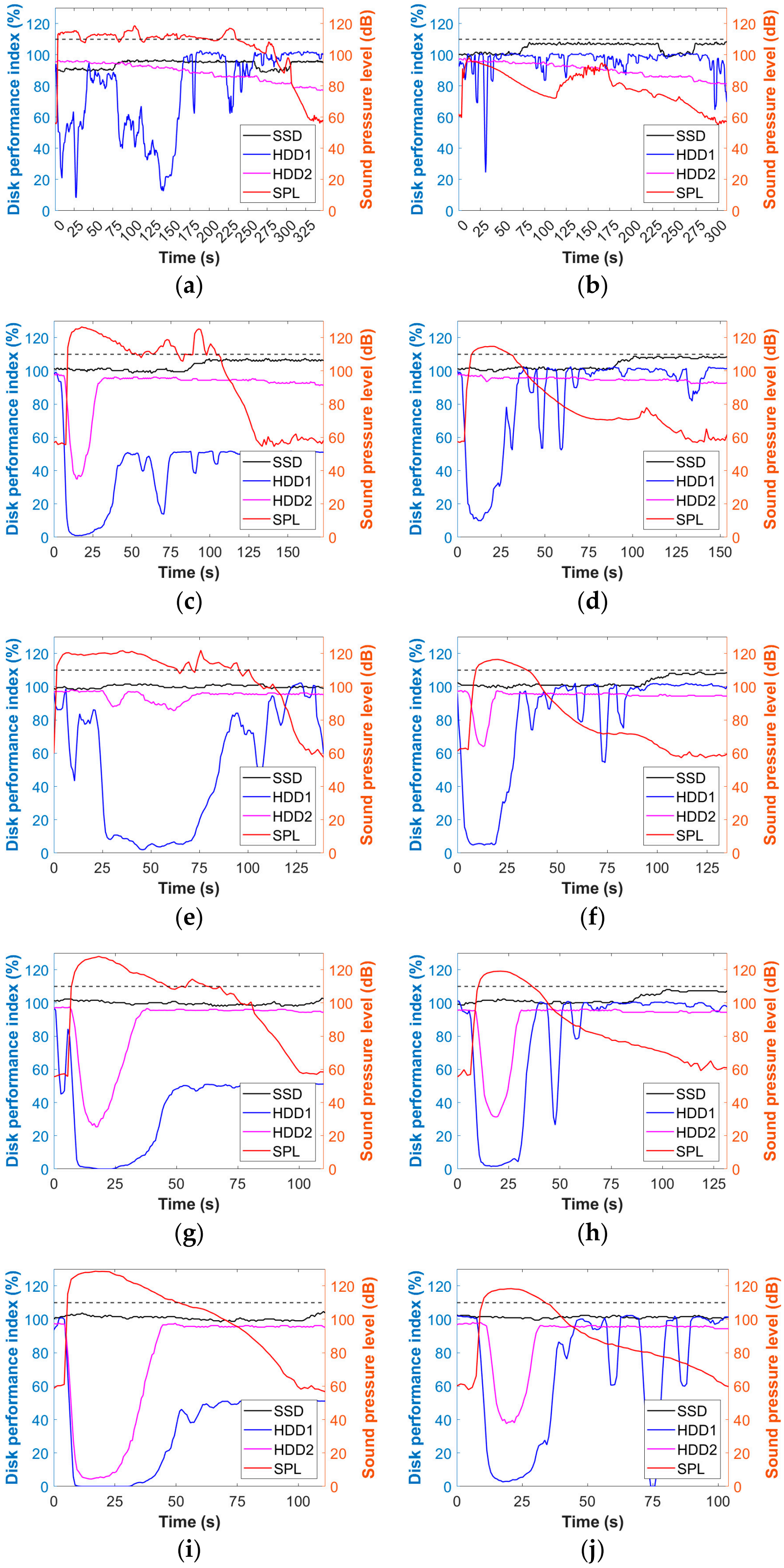

Figure 7. SPL and disk performance index as a function of time throughout a nitrogen IG100 discharge by (**a**) standard and (**b**) silent nozzle with 5 mm orifice diameter; (**c**) standard and (**d**) silent nozzle with 10 mm orifice diameter; (**e**) standard and (**f**) silent nozzle with 14 mm orifice diameter; (**g**) standard and (**h**) silent nozzle with 17 mm orifice diameter; (**i**) standard and (**j**) silent nozzle with 23 mm orifice diameter.

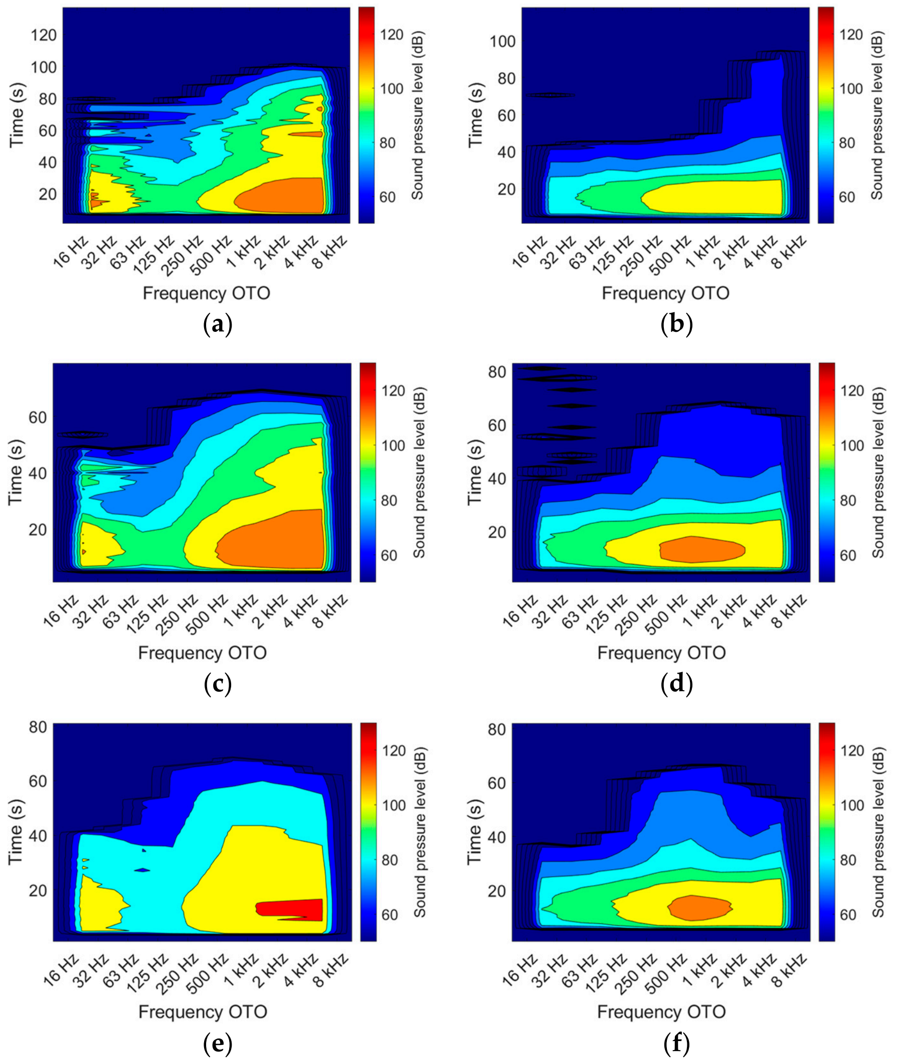

Figure 8. SPL as a function of time and OTO (One-Third Octave bands) frequency throughout a nitrogen IG100 discharge by (**a**) standard and (**b**) silent nozzle with 10 mm orifice diameter; (**c**) standard and (**d**) silent nozzle with 17 mm orifice diameter; (**e**) standard and (**f**) silent nozzle with 23 mm orifice diameter.

When comparing hard drive performance, the difference between configurations with the standard nozzle and those with the silent ones is highlighted by HDD performance index trends. As expected, solid-state storage devices (i.e., SDD) are almost not affected by external noise, hence SDD performance was close to 100% throughout each conducted experiment (Figure 7). The exhibited mild oscillations—in some instances even leading to performance higher than the nominal one (i.e., greater than 100%)—appear unrelated to the actual experimental conditions. On the other hand, HDD performance decay is highly consistent with SPL exceeding the 110 dB threshold; moreover, the higher the SPL, the greater the performance decay (Figure 7). This observation is particularly emphasized by HDD1, which is the hard drive featuring the smaller rate of rotation, and consequently, the lower nominal speed (Table 2); HDD2 seemed less affected by noise, to the point of having its performance almost unaffected by SPL lower than 120 dB and also by noise regrowth for a short timespan (Figure 7c,g). It is also worth noting that HDD1 did not recover its performance level under undisturbed conditions as noise fell below the threshold, due to the discharge by the standard nozzle approaching the end of the process (Figure 7c,g,i); this phenomenon never appeared in tests run with silent nozzles instead. This prolonged performance loss occurring with the discharge produced by standard nozzles with large orifice diameters is arguably due to SPL being above 100 dB at frequencies greater than

4 kHz over a wide portion of the discharge event (Figure 8a,c,e). As previously reported, Dutta suggests that hard drives are affected by SPLs as low as 105 dB in the 4–10 kHz band [31], which may explain the result of only partial recovery even when noise fell below 110 dB. The diagram of Figure 9 serves as an overview of the impact of noise from the tested nozzles on hard drives: (maximum) performance loss is plotted against maximum SPL reached for each tested condition, including both standard and silent nozzle experiments. An apparent correlation between HDD read/write speed and noise appears from the performance dataset, with HDD performance becoming lower as SPL increases. The linear best-fitting curve, applied to each database related to the three tested hard drives, emphasizes that noise is more impactful against the HDD featuring lower nominal speed with respect to those with higher rates of rotation.

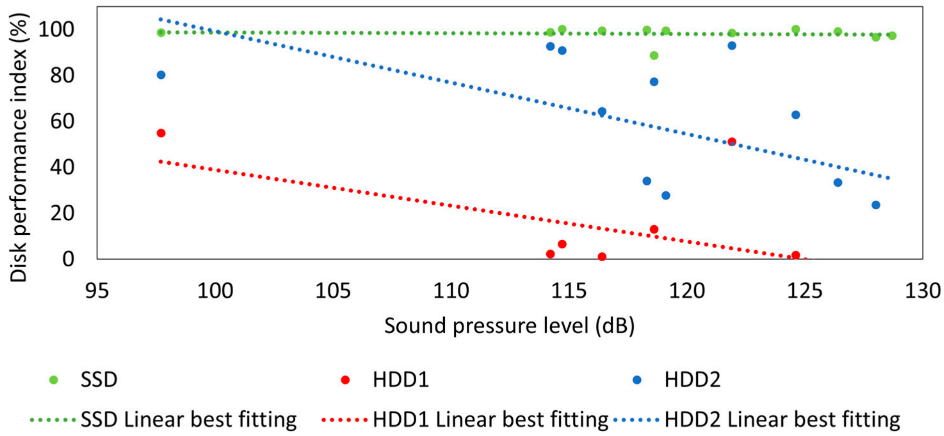

Figure 9. Performance index as a function of maximum SPL reached in every tested condition with nitrogen IG100.

3.2. Discharge of Halocarbon Compounds: Effect of Generated Noise

As reported in Sections 1 and 2.1, one of the scopes of the present work was comparing the discharge of the two types of clean agents in terms of emitted noise, which prompted us to test FK-5-1-12 as a representative of halocarbon compounds. The higher cost associated with these agents—also noted as a drawback by DiNenno [2]—led us to run experiments only against one configuration (Table 3), obviously through both standard and silent nozzles (for low ceiling applications). The trends of SPL and disk performance index are shown for representative tests in Figure 10. The overall consistency of these results with the dataset for the nitrogen IG100 discharge through nozzles of similar orifice size (5 mm, Figure 7a,b) seems to somewhat substantiate a statement provided in a well-recognized white paper [4]: *"The agent used in an extinguishing solution doesn't define per-se the noise level of the system overall"*. However, it is also worth noting that FK-5-1–12 mass flow rate released through a 6 mm diameter nozzle is remarkably larger than that of nitrogen IG100 through a 5 mm diameter nozzle; in fact, the former is close to nitrogen IG100 mass flow rate issued by a 23 mm diameter nozzle (Figure 7i,j), due to its higher density. Even though the released volumetric flow rate can be assumed to be very similar, it appears that almost the same noise is generated by a larger mass flow rate of FK-5-1-12 as that generated by a smaller mass flow rate of nitrogen IG100, when the discharge is operated at the same pressure.

The ability of silent nozzles to reduce noise down to harmless levels is also proven by both the profile of disk performance index (Figure 10) and by SPL presented as a function of frequency, as in the maps of Figure 11. Solid-state drives are obviously not affected, and neither are HDDs with high rates of rotation (i.e., HDD2) if orifice diameter is smaller than 10 mm, yet HDDs with lower speed (i.e., HDD1) exhibit a considerable decay in their performance if standard nozzles are used to release halocarbon compounds, as opposed to the discharge produced by silent ones. However, a remarkable effect can be observed in the results from tests with the silent nozzle (Figures 10b and 11b): SPL shows a sharp decrease after the expected peak upon the onset of discharge (Section 3.1), then followed by another increase up to a plateau-like condition.

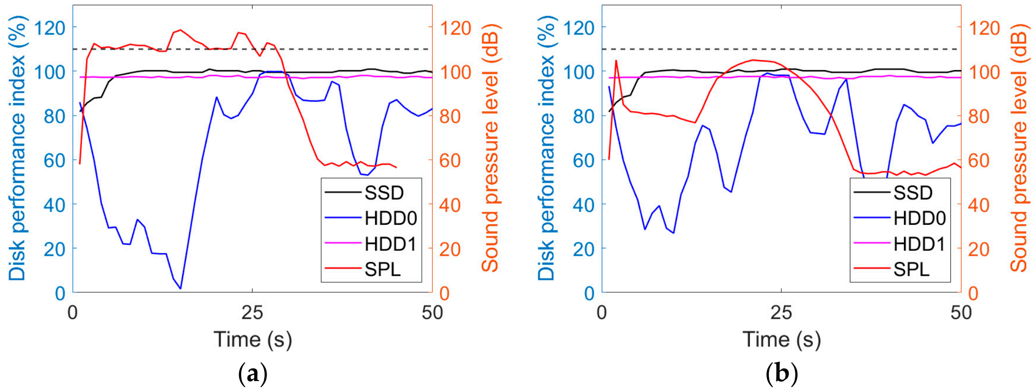

Figure 10. SPL and disk performance index as a function of time throughout FK-5-1-12 discharge by (**a**) standard and (**b**) silent nozzle for low ceiling applications with 6 mm orifice diameter.

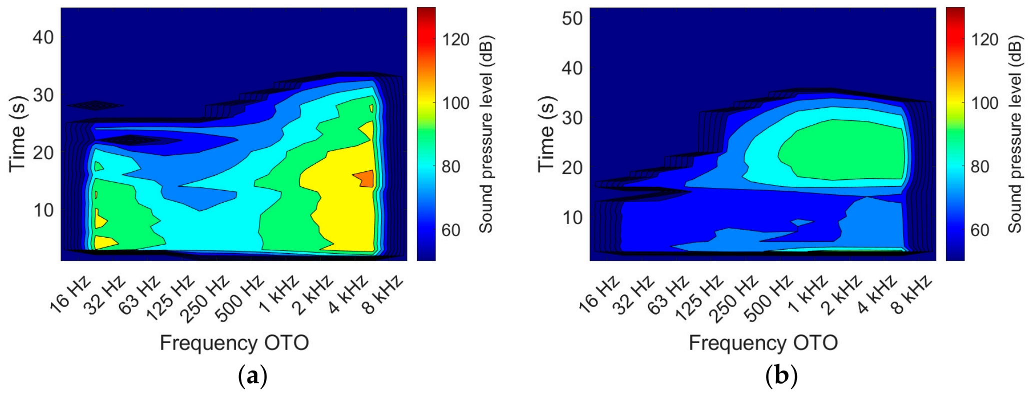

Figure 11. SPL as a function of time and OTO (One-Third Octave bands) frequency throughout FK-5-1-12 discharge by (**a**) standard and (**b**) silent nozzle for low ceiling applications with 6 mm orifice diameter.

This trend is arguably typical of the discharge of liquified gases such as FK-5-1-12, where another gas is also added to superpressurize the agent (i.e., nitrogen, Section 2.1). Firstly, the liquid phase (i.e., FK-5-1-12) is released; as the agent becomes almost exhausted, the discharge becomes nitrogen-laden. Thus, in this last part of the discharge, the Reynolds number changes as a result of a change in the released chemical substance, which reflects the involved thermophysical properties. The tested silent nozzles demonstrated a more effective damping action on the noise emitted through the actual FK-5-1-12 discharge (first phase), whereas the trend already observed in tests with nitrogen IG100 (e.g., Figure 7d,f,h,j) occurred once the gas used to superpressurize the agent was finally released (second phase). This outcome—also shown by the high-frequency (i.e., 1–4 kHz) SPL dataset of Figure 11b—suggests a certain dependence of the sound-absorbing performance on the clean agent type.

3.3. Overview of the Relationship between Flow Rate and Noise

Aiming at a deeper understanding of the effect of released flow rate on the noise emitted by nozzles used in gas-based fire suppression, the SPL dataset was related to mass flow rate calculated by the approach proposed in Section 2.2. The results are presented in Figure 12 for both standard and silent nozzles, those designed for low ceiling applications are included with regard to FK-5-1-12 discharge. As already apparent from the list of tested configurations (Table 3), most of the data are available for standard and silent nozzles with nitrogen IG100 discharge, whereas datasets for the other investigated conditions (i.e., all those involving FK-5-1-12 discharge) consist of a smaller population. Therefore, the degree of statistical significance varies between datasets. Data are plotted in Figure 12 with reference to the employed orifice diameter; the best-fitting curve was also generated as a power law ($y = ax^b$) and is also included in the plots. While formulating the fitting curve, SPL values below 60 dB were discarded, as they were considered almost white noise, and so were flow rate values below 0.15 kg/s, since measurements of the various involved parameters (e.g., pressure, temperature, mass) were deemed unreliable at the onset of the discharge as a result of the steep transient growth. The values of scaling factor a and exponent b are presented in Table 4 for each analyzed condition.

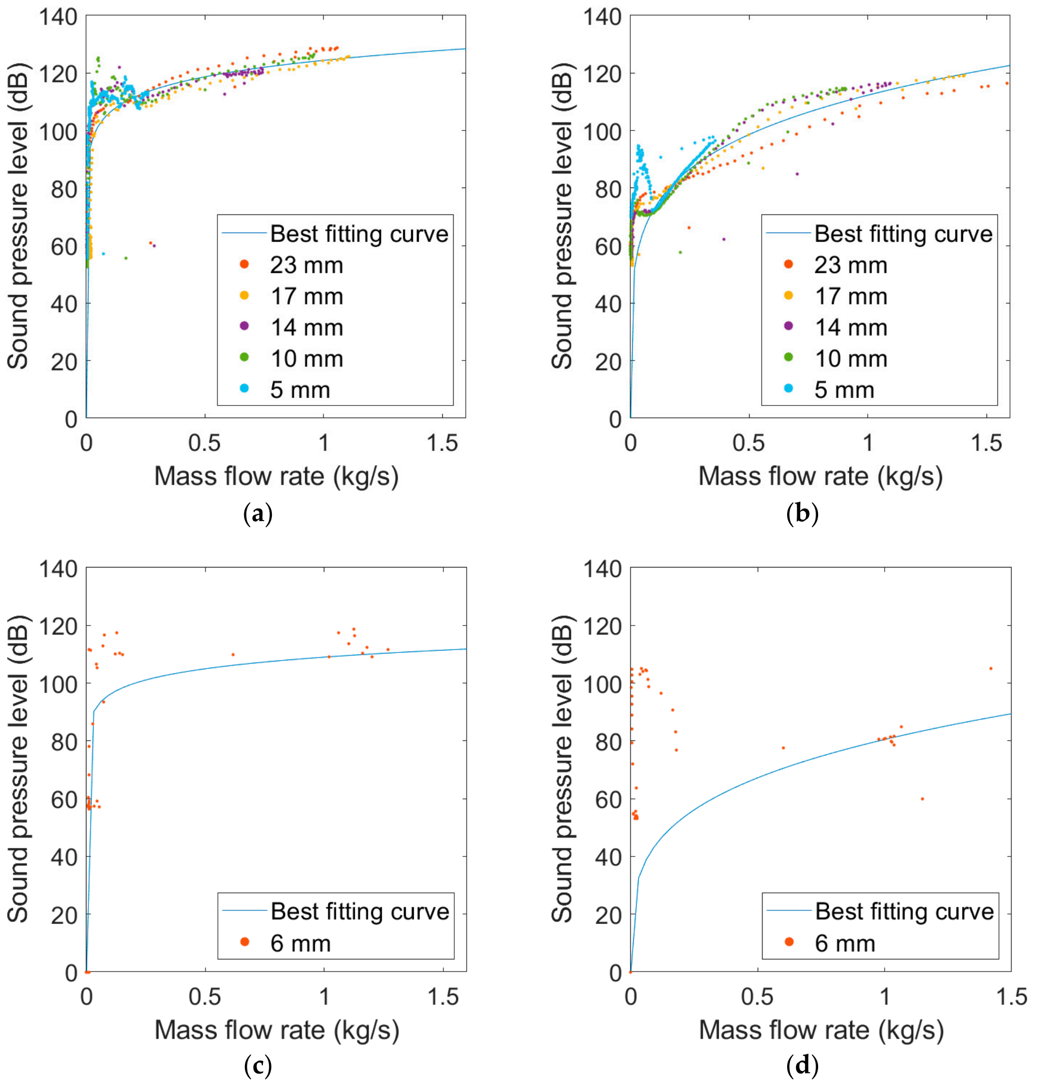

Figure 12. SPL as a function of released mass flow rate, with data points (referred to orifice diameter) and best-fitting curve: (**a**) standard nozzle and nitrogen IG100 discharge; (**b**) silent nozzle and nitrogen IG100 discharge; (**c**) standard nozzle and FK-5-1-12 discharge; (**d**) silent nozzle for low ceiling applications and FK-5-1-12 discharge.

The noise-damping effect of silent nozzles is evident in the diagrams of Figure 7. Moreover, it is worth observing that the larger the released mass flow rate, the higher the emitted noise, a result that holds for all the tested conditions and previously discussed in Section 3.1. However, and rather interestingly, the profiles suggest that the emitted noise has an ever-decreasing growth, evidence of which is also shown by the best-fitting curves and their decreasing slope as mass flow rate increases. This observation also indirectly arises from SPL trends shown in Figure 7: the peaks exhibit similar values as orifice diameter shifts towards the larger sizes, regardless of whether standard (Figure 7g,i) or silent (Figure 7h,j) nozzles are employed. This behavior is consistent with the discussion proposed in Sections 3.1 and 3.2 with regard to the relationship between noise and Reynolds number, which hints at turbulence intensity of the issued jet: as fully developed turbulence is approached, the emitted noise tends to increase under a milder slope. The comparison of Figure 12c and Figure 12b,d suggests that FK-5-1-12 generally yields lower SPL than nitrogen IG100, which is consistent with the findings described in Section 3.2: higher mass flow rate of FK-5-1-12 generates approximately the same noise as a lower mass flow rate of nitrogen IG100, since FK-5-1-12 density is higher than nitrogen density. Even though the datasets are of different size, as previously remarked, and the gap in terms of emitted noise is perceivable, yet mild (i.e., in the order of 10–20 dB, considering standard and silent nozzles), it appears that the different values of the involved thermophysical properties (i.e., density and viscosity) make FK-5-1-12 discharge generate lower noise than nitrogen IG100 discharge, under the same released mass flow rate. On the other hand, the generated noise is rather similar under the same released volumetric flow rate.

Table 4. Constant scaling factor and exponent for the fitting curves generated through a power law formulation.

Tested Condition (Nozzle Type, Clean Agent)	Scaling Factor *a*	Exponent *b*
Standard, nitrogen IG100	124.4	0.06788
Silent, nitrogen IG100	112.3	0.1873
Standard, FK-5-1-12	109	0.05422
Silent for low ceiling applications, FK-5-1-12	80.49	0.2596

4. Conclusions

Most hard drives are subject to performance decay as noise beyond a certain threshold —usually identified as 110 dB [4,16–20]—reaches them. The problem is particularly relevant when fire protection of data centers is involved, since gas-based suppression systems are widely employed for this purpose: the noise emitted by the nozzles through a discharge of the selected clean agents (i.e., inert gases or halocarbon compounds) is well-known to damage the electronic equipment within the compartment. Hence, silent nozzles are designed and often used to address this undesired effect; however, the open literature currently offers few scientific studies on the subject. Arguably an unprecedented effort, an experimental approach was devised and developed to quantitatively assess the noise generated by both standard and silent nozzles in a comparative fashion, together with the performance decrease in the hard drives throughout several discharge conditions. To this end, a preliminary evaluation of repeatability and ability to properly capture the involved phenomena was carried out against the proposed experimental setup and methodology. Notably, the employed nozzles proved reasonably suitable for applying the point source model [22], thus allowing us to neglect the directionality of the emitted noise. The developed approach may be expanded by repeating the same measurements (i.e., sound pressure level and performance decay) at various angular locations, following the guidance from a previous work [15], which applies the here-presented setup as a reference to evaluate acoustic performance of virtually any nozzle for gas-based suppression system. A series of experiments were conducted, mostly releasing nitrogen IG100, but also FK-5-1-12, which allowed a comparison between the two types of clean agents. Constant pressure was imposed throughout a large portion of each discharge event using constant flow valves; various orifice diameters were tested, which translates into variations in the released flow rate. Moreover, three hard drives were used as targets to test their performance over a discharge event: two HDDs with different rates of rotation and one SSD, which was almost unaffected by external noise.

As expected, silent nozzles proved capable of limiting the generated noise down to values less harmful to hard drives. Notably, each discharge—whether produced by standard or silent nozzles—exhibited an increase in the emitted noise up to a maximum from its onset, usually followed by a plateau-like trend and the final decay. Fluctuations occurred possibly as a result of pressure oscillations within the controlled phase (i.e., the release at virtually constant pressure). This behavior hints at the known dependence of sound emitted by gaseous jets flowing through an orifice on turbulence intensity, thus being ultimately correlated to Reynolds number. This relationship also supports the discovered increase in peak noise level as the released flow rate increased (i.e., as larger orifice diameter was employed in the tests). Nevertheless, the difference between the reached noise maxima became less remarkable as the released flow rate increased, which also suggests that once the Reynolds number becomes sufficiently high that fully developed turbulence be reached, noise intensity increases along a milder slope. Rather interestingly, the recorded performance decay of the target HDD qualitatively followed the noise trend, yet the HDD featuring the lower read/write speed appeared remarkably more affected than that with the higher rate of rotation. Notably, the former exhibited instances of partial performance recovery as noise decreased as the discharge event approached its end, which emphasized the need for conducting spectral analysis of the emitted sound. It was observed that noise emitted at a higher frequency (4–8 kHz) could reach values above 100 dB even in the last part of the discharge event: as found by Dutta [31], such noise intensity in this band can be detrimental to HDD performance, even though it is lower than 110 dB. With regard to the comparison between the two clean agent types, a similar behavior could be inferred by comparing results from nitrogen IG100 and FK-5-1-12 discharge. However, a noise regrowth was observed as silent nozzles were employed in the latter case, which is arguably related to the discharge of the superpressurizing agent (i.e., nitrogen) added within the tank, once the halocarbon compound is fully released. This second phase proved consistent with inert gas discharge in terms of emitted noise, yet also suggested a better noise-damping effect on FK-5-1-12 by silent nozzles than on nitrogen. The commonly accepted independence of generated noise from the released agent is also supported by the acquired dataset when referring to volumetric flow rate (i.e., orifice diameter of similar size and same discharge pressure). However, the discharge of a stronger FK-5-1-12 mass flow rate generates almost the same noise as that of a lower mass flow rate of nitrogen IG100, which is consistent with the former having higher density. The difference in the values of the involved thermophysical properties (i.e., density and viscosity) impacts on Reynolds number of the two jets and ultimately on the emitted noise as they pass through an orifice.

The present work sheds light on the acoustical performance of nozzles employed in gas-based fire protection in relation to several design parameters (i.e., selected clean agent type, flow rate, orifice diameter); moreover, it proposes an approach to compare nozzles in terms of emitted noise. Overall, both the results and the methodology may be of interest for nozzle and fire protection system designers, as well as provide a foundation for further research on specific aspects of the involved phenomena (e.g., quantitative relationship between noise and turbulence intensity, potential supersonic-to-subsonic transition through the discharge). Further research may arise out of this work towards investigating the combined action of several nozzles—either standard or silent—at the same time, in terms of generated noise (i.e., superposition of waves and interference) and impact on HDDs. Moreover, the here-proposed methodology can be employed to expand the variety of tested silent nozzles, which may include new structures such as sound-absorbing layers (e.g., honeycomb porous shells [32]).

Author Contributions: Conceptualization, L.T. and P.E.S.; methodology, N.T., L.T. and P.E.S.; formal analysis, M.S., N.T., L.T. and P.E.S.; investigation, M.S., N.T., L.T. and P.E.S.; resources, L.T.; writing—original draft preparation, P.E.S.; writing—review and editing, N.T. and P.E.S.; supervision, P.E.S.; project administration, L.T. and P.E.S.; funding acquisition, L.T. All authors have read and agreed to the published version of the manuscript.

Funding: This study was partially funded by Regione Emilia-Romagna, Italy through the POR-FESR 2014-2020 program, as a part of the FIRESOFT—*Piattaforma software di modellazione, testing e validazione in-house di impianti antincendio fissi* project, grant agreement (CUP code) no. E85F19001860007.

Institutional Review Board Statement: Not applicable.

Informed Consent Statement: Not applicable.

Data Availability Statement: Not applicable.

Acknowledgments: The authors wish to thank the technical staff of Bettati Antincendio S.r.l., Italy for providing assistance in assembling the experimental setup.

Conflicts of Interest: The authors declare no conflict of interest.

References

1. Grant, C.C. Halon design calculations. In *SFPE Handbook of Fire Protection Engineering*; DiNenno, P.J., Drysdale, D., Beyler, C.L., Walton, W.D., Custer, R.L.P., Hall, J.R., Jr., Watts, J.M., Jr., Eds.; National Fire Protection Association: Quincy, MA, USA, 2002; Section 4, Chapters 4–6; pp. 149–172.
2. DiNenno, P.J. Halon replacement clean agent total flooding systems. In *SFPE Handbook of Fire Protection Engineering*; DiNenno, P.J., Drysdale, D., Beyler, C.L., Walton, W.D., Custer, R.L.P., Hall, J.R., Jr., Watts, J.M., Jr., Eds.; National Fire Protection Association: Quincy, MA, USA, 2002; Section 4, Chapters 4–7; pp. 173–200.
3. Kim, Y.-H.; Lee, M.; Hwang, I.-J.; Kim, Y.-J. Noise reduction of an extinguishing nozzle using the Response Surface Method. *Energies* **2019**, *12*, 4346. [CrossRef]
4. Mann, M.T.; Coll, M. *Potential Problems with Computer Hard Disks When Fire Extinguishing Systems Are Released*; Siemens Switzerland: Zug, Switzerland, 2010.
5. Lilley, G.M. Aerodynamic noise—A review of the contributions to jet noise research at the College of Aeronautics, Cranfield 1949-1961 (together with some recent conclusions). *Aeronaut. J.* **1984**, *88*, 213–223.
6. Tam, C.K.W.; Tanna, H.K. Shock associated noise of supersonic jets from convergent-divergent nozzles. *J. Sound Vib.* **1982**, *81*, 337–358. [CrossRef]
7. Tam, C.K.W. Influence of nozzle geometry on the noise of high-speed jets. *AIAA J.* **1998**, *36*, 1396–1400. [CrossRef]
8. Dutta, T.; Barnard, A.R. Performance of hard disk drives in high noise environments. *Noise Control Eng. J.* **2017**, *65*, 386–395. [CrossRef]
9. Green, K.; Nelson, D.; Pai, N.; Nickerson, M. Hard drive performance degradation due to high level noise in data centers. In Proceedings of the 40th International Congress and Exposition on Noise Control Engineering—Inter-Noise, Osaka, Japan, 4–7 September 2011.
10. Nickerson, M.L.; Green, K.; Pai, N. Tonal noise sensitivity in hard drives. *Proc. Meet. Acoust.* **2014**, *20*, 040006.
11. Daigle, B. *Data Centers around the World: A Quick Look*; United States International Trade Commission: Washington, DC, USA, 2021.
12. Loureiro, M.A.; Elder, A.; Ahmadzadegan, A. Acoustic nozzle design for fire protection application. In Proceedings of the 2017 Suppression, Detection, and Signaling Research and Applications Conference (SUPDET 2017) and 16th International Conference on Fire Detection (AUBE'17), College Park, MD, USA, 12–14 September 2017.
13. Kim, Y.-H.; Yoo, H.-S.; Hwang, I.-J.; Kim, Y.-J. Influence of the nozzle contraction angles of gaseous extinguishing systems on discharge noise. *Fire Sci. Eng.* **2019**, *33*, 77–82. [CrossRef]
14. Mihalace, C.-M.; Bigan, C.; Panduru, V.; Tsakiris, C. Modelling of noise reduction for datacentre buildings fire protection with inert gas systems. *MATEC Web Conf.* **2019**, *290*, 12006. [CrossRef]
15. Koushik, S.; McCormick, D.; Cao, C.; Corn, M. Acoustic impact of fire suppression nozzles. In Proceedings of the 2017 Suppression, Detection, and Signaling Research and Applications Conference (SUPDET 2017) and 16th International Conference on Fire Detection (AUBE'17), College Park, MD, USA, 12–14 September 2017.
16. *NFPA 75*; Standard for the Fire Protection of Information Technology Equipment. National Fire Protection Association: Quincy, MA, USA, 2020.
17. *Silence Is Golden—Maintaining the Integrity of HDD's in a Noisy Situation*; Fire Eater: Hillerød, Denmark, 2016.
18. *Effect of Sound Waves on Data Storage Devices*; Fire Suppression Systems Association: Baltimore, MD, USA, 2018.
19. Sandahl, D.; Elder, A.; Barnard, A. *Impact of Sound on Computer Hard Disk Drives and Risk Mitigation Measures*; Form no. T-2016367-01; Johnson Controls: Milwaukee, WI, USA, 2018.
20. *Silent Extinguishing*; Siemens Switzerland: Zug, Switzerland, 2022.
21. Silva, R.A.; Buiatti, C.M.; Cruz, S.L.; Pereira, J.A.F.R. Pressure wave behaviour and leak detection in pipelines. *Comput. Chem. Eng.* **1996**, *20*, 5491–5496. [CrossRef]
22. Li, K.M.; Waters-Fuller, T.; Attenborough, K. Sound propagation from a point source over extended-reaction ground. *J. Acoust. Soc. Am.* **1998**, *104*, 679. [CrossRef]
23. Coleman, H.W.; Steele, W.G. *Experimentation and Uncertainty Analysis for Engineers*; Wiley: New York City, NY, USA, 1999.
24. Tilton, J.N. Fluid and particle dynamics. In *Perry's Chemical Engineers' Handbook*; Perry, R.H., Green, D.W., Eds.; McGraw-Hill: New York City, NY, USA, 1997; Section 6; pp. 1–54.
25. CoolProp. Available online: http://www.coolprop.org/ (accessed on 24 August 2022).

26. Santangelo, P.E.; Jacobs, B.C.; Ren, N.; Sheffel, J.A.; Corn, M.L.; Marshall, A.W. Suppression effectiveness of water-mist sprays on accelerated wood-crib fires. *Fire Saf. J.* **2014**, *70*, 98–111. [CrossRef]
27. Santangelo, P.E.; Tarozzi, L.; Tartarini, P. Full-scale experiments of fire control and suppression in enclosed car parks: A comparison between sprinkler and water-mist systems. *Fire Technol.* **2016**, *52*, 1369–1407. [CrossRef]
28. Cannio, M.; Righi, S.; Santangelo, P.E.; Romagnoli, M.; Pedicini, R.; Carbone, A.; Gatto, I. Smart catalyst deposition by 3D printing for Polymer Electrolyte Membrane Fuel Cell manufacturing. *Renew. Energy* **2021**, *163*, 414–422. [CrossRef]
29. Mi, J.; Xu, M.; Zhou, T. Reynolds number influence on statistical behaviors of turbulence in a circular free jet. *Phys. Fluids* **2013**, *25*, 075101. [CrossRef]
30. White, F.M. *Viscous Fluid Flow*; McGraw-Hill: New York City, NY, USA, 2006.
31. Dutta, T. Performance of Hard Disk Drives in High Noise Environments. Master's Thesis, Michigan Technological University, Houghton, MI, USA, 2017.
32. Thongchom, C.; Jearsiripongkul, T.; Refahati, N.; Roudgar Saffari, P.; Roodgar Saffari, P.; Sirimontree, S.; Keawsawasvong, S. Sound transmission loss of a honeycomb sandwich cylindrical shell with functionally graded porous layers. *Buildings* **2022**, *12*, 151. [CrossRef]